Neuron, Volume *59*
Supplemental Data

Extent of voltage sensor movement during gating of Shaker K^+ channels

David J. Posson and Paul R. Selvin

Evaluation of Four-Exponential Fit Distance Determination by Analysis of Simulated Data

We performed simulations to test the accuracy of the multi-distance determinations of the constrained four exponential fit (described in Methods) used to analyze VSD to CTX experiments. We picked five alpha carbon positions on the Kv1.2 chimera VSD structure (pdb code: 2r9r) and measured the distances to a theoretical acceptor position 7.5 Å or 10 Å from the symmetry axis and above the charybdotoxin peptide (Supplementary Figure S1). Simulated data is generated by assuming a bi-exponential donor probe that has a dominant component (75% amplitude) with 1600 μs lifetime and a minor component (25% amplitude) with 300 μs lifetime. The simulation acceptor is BodipyFl (used in our experiments for S2-S4) with an Ro=39 Å for the dominant donor component and an Ro=29.5 Å for the minor donor component. For example, in the case of Cα 294, the dominant donor component gives four amplitudes and time constants: A_1 = 80.1, τ_1 = 88.4 μs; A_2 = 28.3, τ_2 = 227.3 μs; A_3 = 12.5, τ_3 = 435.3 μs; A_4 = 6.9, τ_4 = 649.4 μs. The minor donor component gives four amplitudes and time constants: A_1^* = 26.7, τ_1^* = 71.4 μs; A_2^* = 9.4, τ_2^* = 140.8 μs; A_3^* = 4.2, τ_3^* = 199.9 μs; A_4^* = 2.3, τ_4^* = 235.4 μs. The minor components are a factor of 3 smaller in amplitude than the dominant contributions. A realistic amount of random noise is added to the simulated fluorescence signal (Figure S2). The simulated data is then fit to the four exponential fit function (as was the experimental data: $A [k_1 \exp(-t/\tau_1) + k_2 \exp(-t/\tau_2) + k_3 \exp(-t/\tau_3) + k_4 \exp(-t/\tau_4)]$, where $\tau_n = \tau_D(d_n^6/(d_n^6 + R_o^6))$ and $k_n = 1/\tau_n - 1/\tau_D$ with τ_D = 1600 μs and R_o = 39 Å for Tb to BodipyFl) and the accuracy is quantified by calculation of the % difference between the fitted distances and the theoretical distances. The fits show that the minor donor populations can safely be ignored and the distances can be extracted with the four exponential fit using the constraints given by the pyramid geometry model presented. 10 simulations, representing 40 distance determinations, resulted in an average error (See Table S1) of 3.9 ± 2.3% (std. dev.).

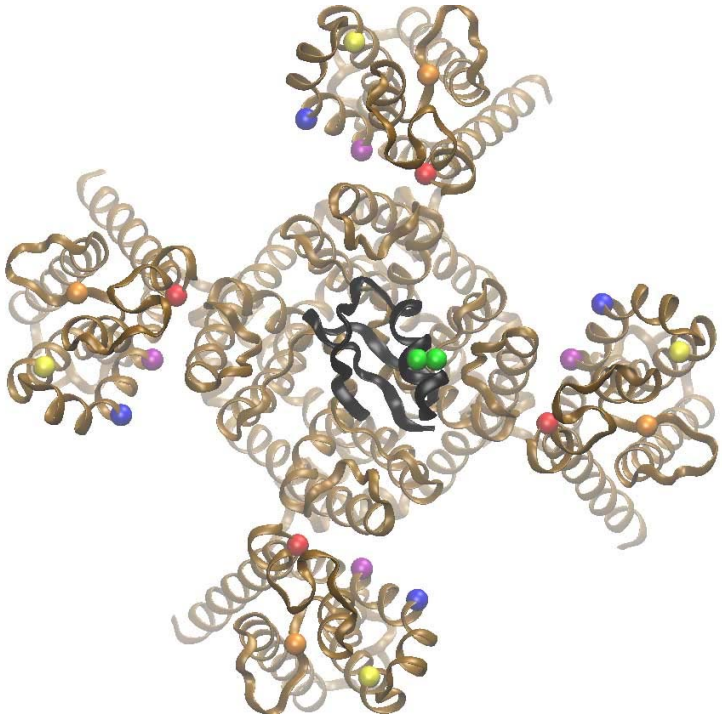

Supplementary Figure S1. Kv1.2 chimera structure (brown) with bound charbydotoxin (black). Positions used for distance-determination simulations are highlighted. The modeled acceptor positions are shown in green, 7.5 and 10.0 Å from the channel symmetry axis. The alpha carbon positions used for simulated donor positions are 184 (red), 213 (orange), 273 (yellow), 287 (blue), and 294 (purple).

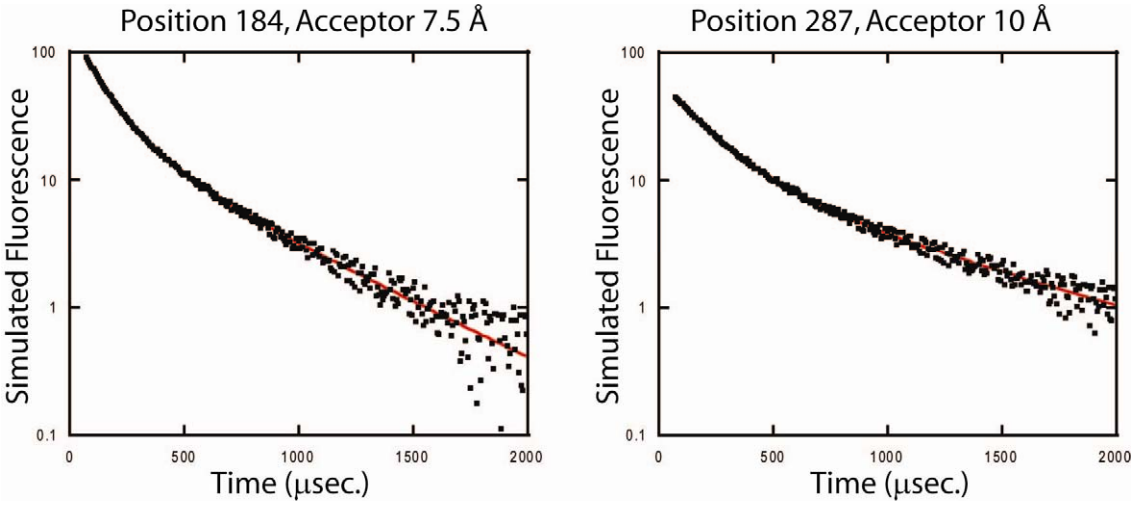

Supplementary Figure S2. Two example fluorescence data simulations of the four donor-acceptor distances with bi-exponential donor are shown. The red line represents the best fit using the constrained four-exponential fit described in Methods.

Site	Theoretical Distances, Acceptor 7.5 Å	Distances from Fit	% error	Theoretical Distances, Acceptor 10 Å	Distances from Fit	% error
184	24.3	24.091	1.023	22.6	22.164	1.972
	28.9	27.312	5.331	28.9	26.95	6.650
	33.1	32.761	1.054	34.4	33.496	2.627
	36.6	35.197	3.911	38.9	36.838	5.203
213	34.4	32.817	4.684	32.2	30.583	5.051
	40.3	43.247	-7.259	40.3	40.614	-0.754
	43.5	43.247	0.627	44.5	40.614	8.773
	48.3	51.611	-6.81	50.7	48.618	4.088
273	38.2	36.119	5.521	35.9	33.966	5.466
	45.69	46.802	-2.433	46.1	44.217	4.105
	46	46.802	-1.721	46.5	44.217	4.991
	52.4	55.464	-5.908	54.8	52.503	4.156
287	30.2	28.879	4.374	28.2	27.514	2.363
	35.9	35.036	2.270	35.9	34.576	3.795
	38.9	37.947	2.324	39.9	42.753	-7.204
	43.4	42.819	1.315	45.7	47.606	-4.169
294	30.3	28.975	4.499	28.7	27.861	2.923
	36.7	35.987	1.809	37.2	34.358	7.739
	36.7	35.987	1.809	37.2	40.114	-7.688
	42	41.84	0.428	44.2	44.871	-1.609

Table S1. Results of 10 data simulations and fit to constrained four exponential fit. The resulting 40 distances are determined with ~4% error from the theoretical. Therefore, our fit function can accurately determine four simultaneous distances even in the presence of a minor donor component that is not taken into account in the analysis.

Comparison of S4 models in the resting VSD

The simple model presented in the text (Figure 7C) for a resting-state VSD was based on the position of the S4-S5 linker in the recently solved MloK1 structure (Clayton et al., 2008). MloK1 is likely a non-voltage sensing channel due to the absence of arginines in the homologous positions to the gating charges of Kv channels. However, the S4-S5 linker is in a position that constrains the S6 gate in a KcsA-like bundle crossing conformation, indicative of a closed channel. We aligned the Kv1.2 chimera S4/S4-S5 linker based on a structural alignment between the S4-S5 linkers (chimera residues 307-319 with MloK1 residues 112-124). This model of the closed-state position of S4 assumes that in Kv1.2: the pore domain and S4-S5 linker take a conformation similar to that seen in the MloK1 structure and that the S4 and S4-S5 linker do not change their relative conformations between closed and open, moving as a rigid body.

Two other models of the S4 closed-position have been published recently. The first, based on structural constraints derived from experiments using the KAT1 channel, reported a change in z-axis for the top of S4 to be 12-15 Å (Grabe et al., 2007). This movement is twice as large as the S4 change reported in our study and therefore seems inconsistent with LRET. The

second study, based on a multitude of functional data on Shaker, reports a vertical S4 movement of 7 ± 5 Å for the entire helix (7-10 Å for the gating charge positions), see Supplementary information in (Pathak et al., 2007). Therefore, this movement is similar to our LRET results, though may be slightly larger overall. We show a comparison between these three models for the down state of S4 in Supplementary Figure S3.

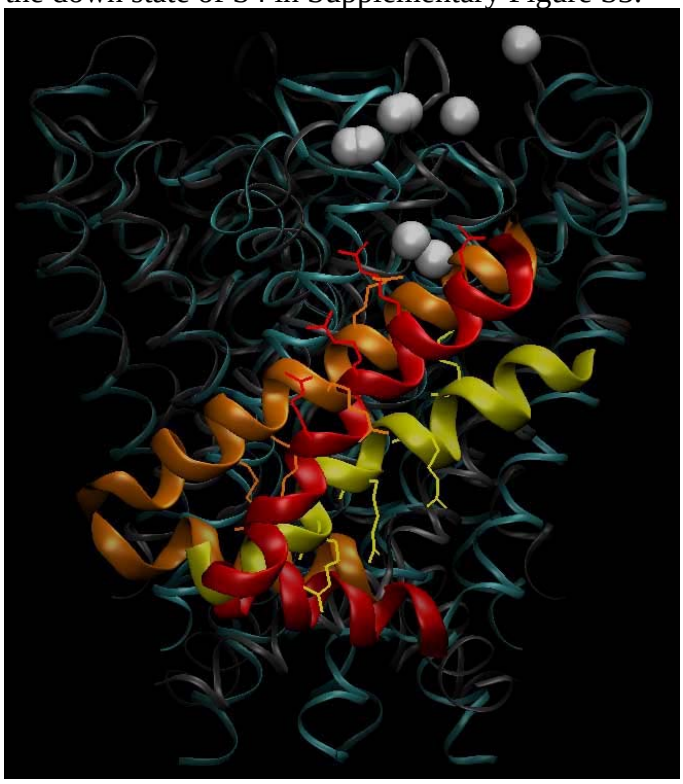

Supplementary Figure S3. Three models of S4 in the down-state are shown along with closed pore domains. The grey pore-domain and orange S4/S4-S5 linker is from the Kv1.2 closed model of Yarov-Yarovoy and coworkers. The cyan pore-domain is the pore from the MloK1 structure. The S4/S4-S5 linker in red is the simple model presented in our study using an alignment of Kv1.2 S4-S5 linker with the linker from the MloK1 structure. The yellow S4 is the model of Grabe and coworkers. All models are compared based on alignment with selectivity filter coordinates. The white spheres are the estimated Tb^{3+} locations for LRET experiments on the 9 Shaker residues above the first gating charge, R1. The modest change in our simple model (red) is similar to that of Yarov-Yarovoy and coworkers (Supplementary Table S2) and consistent with our LRET results. Our simple model does not include the likely twist or reorientation of S4 that likely helps position the gating charges inward (gating charge positions are highlighted in all models).

Gating Charge Position	Posson Model Vertical Change (Å)	Yarov-Yarovoy Model Vertical Change (Å)	Grabe Model Vertical Change (Å)
R1	6.7	10.5	14.4
R2	6.4	11.7	15.4
R3	6.1	9.8	13.4
R4	5.7	6.5	12.6

Table S2. Vertical change of the alpha carbons for gating charge positions (referred to as R1-R4) between the closed models discussed and the open Kv1.2 chimera structure. The simple model we have presented best agrees with our change from LRET. The model of Yarov-Yarovoy best fits the internal constraints determined for the VSD, including a likely twisting of S4.

Clayton, G. M., Altieri, S., Heginbotham, L., Unger, V. M., and Morais-Cabral, J. H. (2008). Structure of the transmembrane regions of a bacterial cyclic nucleotide-regulated channel. Proc Natl Acad Sci U S A *105*, 1511-1515.

Grabe, M., Lai, H. C., Jain, M., Jan, Y. N., and Jan, L. Y. (2007). Structure prediction for the down state of a potassium channel voltage sensor. Nature *445*, 550-553.

Pathak, M. M., Yarov-Yarovoy, V., Agarwal, G., Roux, B., Barth, P., Kohout, S., Tombola, F., and Isacoff, E. Y. (2007). Closing in on the resting state of the Shaker K(+) channel. Neuron *56*, 124-140.